Current Microbiology (2023) 80:238
https://doi.org/10.1007/s00284-023-03342-9

Deciphering Interactions Within a 4-Strain Riverine Bacterial Community

Mathias Bonal[1,2] · Lise Goetghebuer[1] · Clémence Joseph[2] · Didier Gonze[3] · Karoline Faust[2] · Isabelle F. George[1,4]

Received: 13 September 2022 / Accepted: 23 May 2023

Abstract

The dynamics of a community of four planktonic bacterial strains isolated from river water was followed in R2 broth for 72 h in batch experiments. These strains were identified as *Janthinobacterium* sp., *Brevundimonas* sp., *Flavobacterium* sp. and *Variovorax* sp. 16S rRNA gene sequencing and flow cytometry analyses were combined to monitor the change in abundance of each individual strain in bi-cultures and quadri-culture. Two interaction networks were constructed that summarize the impact of the strains on each other's growth rate in exponential phase and carrying capacity in stationary phase. The networks agree on the absence of positive interactions but also show differences, implying that ecological interactions can be specific to particular growth phases. *Janthinobacterium* sp. was the fastest growing strain and dominated the co-cultures. However, its growth rate was negatively affected by the presence of other strains 10 to 100 times less abundant than *Janthinobacterium* sp. In general, we saw a positive correlation between growth rate and carrying capacity in this system. In addition, growth rate in monoculture was predictive of carrying capacity in co-culture. Taken together, our results highlight the necessity to take growth phases into account when measuring interactions within a microbial community. In addition, evidence that a minor strain can greatly influence the dynamics of a dominant one underlines the necessity to choose population models that do not assume a linear dependency of interaction strength to abundance of other species for accurate parameterization from such empirical data.

Introduction

Riverine microbial communities represent key components of lotic ecosystems, as they carry out a number of important functions such as recycling of organic matter or degradation of pollutants [1, 2]. For the past decades, fingerprinting techniques and next-generation sequencing technologies have allowed microbiologists to detect specific taxa and correlate them with such processes [3–5]. Their studies revealed that for instance, abundant bacteria belonging to the genus *Flavobacterium* are involved in typical organic matter degradation pathways like polysaccharide decomposition [6], whereas less abundant bacteria such as *Variovorax* thrive in polluted rivers thanks to their ability to degrade xenobiotics like pesticides [7]. Nevertheless, these studies do not aim for a detailed understanding of the internal functioning of this microbiome. Indeed, microbial community dynamics is governed by a number of factors, which include environmental parameters and/or interactions between community members. In a number of publications, authors infer ecological interactions from presence/absence or abundance of the different taxa (16S rRNA data) in situ [8–10]. Although inferred interactions are in some cases confirmed experimentally and can lead to biological insights [11, 12], the accuracy of interaction networks constructed from abundance data is usually low [13, 14]. Relying on Gause's pioneering work [15], another possibility is to compare growth curves of species in monoculture with those in co-cultures. By assessing if species in co-culture do better,

✉ Isabelle F. George
isabelle.george@ulb.be

1 Laboratory of Ecology of Aquatic Systems, Brussels Bioengineering School, Université Libre de Bruxelles, 1050 Brussels, Belgium

2 Present Address: Laboratory of Molecular Bacteriology (Rega Institute), Department of Microbiology, Immunology and Transplantation, KU Leuven, 3000 Louvain, Belgium

3 Unit of Theoretical Chronobiology, Faculty of Sciences, Université Libre de Bruxelles, 1050 Brussels, Belgium

4 Laboratory of Marine Biology, Department of Biology, Université Libre de Bruxelles, 1050 Brussels, Belgium

Published online: 09 June 2023

equal or worse than in monocultures, the sign and strength of pairwise interactions can be deduced [16–19]. Usually, systematic measurements of growth curves are carried out by quantifying optical density (OD) at wavelengths ranging from 590 to 620 nm [19–22]. However, inference of interactions is problematic when the OD is not scaling linearly with cell number [23]. Yet, interaction networks derived from growth curves based on cell counts are still rare [24, 25]. Accurate elucidation of interaction networks is important to parameterize the mathematical models, which have become important to study key ecological processes affecting microbial communities, such as community assembly, diversity or stability [26–28].

Interaction networks have not been derived experimentally for lotic communities yet. Here, we carried out an explorative study of the interactions within a model microbial community of four planktonic strains isolated from a Belgian river (*Janthinobacterium* sp., *Brevundimonas* sp., *Flavobacterium* sp. and *Variovorax* sp.). This choice was based on several criteria, namely that these strains belong to genera found in rivers worldwide [29–32] and that they have distinct metabolic profiles [21]. Their closest relatives (Table 1) have abilities of interest in the river ecosystem, *e.g.* participation in the sulphur cycle for *Flavobacterium saccharophilum* [6], degradation of persistent pollutants for *Variovorax paradoxus* [33], and persistence in the riverine microbiome thanks to an aptitude to resist to (i) environmental stresses such as protozoan grazing for *Janthinobacterium lividum* [34] and to (ii) antibiotics brought by wastewater treatment plant effluents for *Brevundimonas intermedia* [35]. This variety of profiles makes these strains interesting to study in the context of interactions. In addition, each strain displays a unique morphotype in agar plates, which allows monitoring cross-contaminations in the experiments. We set up an experimental design with mono-, bi- and quadri-cultures to follow the changes in relative and absolute abundances of the bacterial community composition over a period of 72 h. We then measured corresponding pairwise interaction strengths in bi- and quadri-cultures and represented them in two interaction networks, each reflecting how the community members interact with one another, first in exponential phase, then in stationary phase. Additional antagonism tests were performed to further investigate some of these interactions.

Material and Methods

Strain Information and Selection

In a study published in 2017 [21], Goetghebuer and collaborators built up a model river bacterial community composed of 20 strains. 16 of these 20 strains were isolated from the water column of the Zenne river (Belgium). From the 16 strains isolated by Goetghebuer and collaborators, we selected four strains belonging to genera commonly found in rivers: *Janthinobacterium*, *Brevundimonas*, *Flavobacterium* and *Variovorax* [29, 30, 32], to build up a model bacterial community. They were also chosen for the diversity of their individual growth rates, metabolic profiles and ecological functions, as well as for the morphotype they display on R2-agar, easily distinguishable with the naked eye. To ensure that descendent cultures obtained in agar plates coming from the lab's stock were pure, we carried out a genetic identification of colonies of each bacterium cultivated in monoculture. First, DNA was extracted from a pure colony from each strain and the 16S rRNA gene was amplified and sequenced with Sanger method (Macrogen, Netherlands). The sequences were then trimmed and assembled into contigs with DNASTAR (Lasergene, Madison, USA). Contigs were eventually aligned with databases from BLAST (https://blast.ncbi.nlm.nih.gov/Blast.cgi) and SILVA (https://www.arb-silva.de). They were identified as 78R (*Janthinobacterium* sp.), 124Z (*Brevundimonas* sp.), 515Z (*Flavobacterium* sp.) and 1315Z (*Variovorax* sp.) (Table 1) and their sequences were uploaded to the NCBI GenBank database (accession numbers: ON391592 to ON391595).

Experimental Design for Mono- and Co-cultures

We followed the growth of our microbial community in batch experiments incubated at 20 °C using R2 broth (R2B) (Melford, Ipswich, UK). Each of the four strains was first grown separately on R2-agar. Colonies were then transferred into R2B and incubated at 20 °C and 176 rpm for 48 h (pre-cultures). We estimated each pre-culture's cell concentration by flow cytometry (see protocol below) and subsequently diluted each pre-culture in R2B to a concentration of $\approx 10^4$ cells/mL. Two types of co-cultures were assembled: (i) six bi-cultures where strains were cultured pairwise, and (ii) a quadri-culture with the four strains mixed altogether. In both cases, the strains were equally mixed at $t = 0$ h. Each co-culture was incubated in Schott bottles (Duran, UK) in a volume of 1 L of R2B, at 20 °C and 176 rpm. Three biological replicates of each co-culture were run separately (from different pre-cultures, run at different times). An uninoculated 1 L-volume of R2B was monitored as negative control. No contamination was detected in the negative control during the course of the experiments. Aliquots (25 to 50 mL) were collected at eight sampling times (0 h, 18 h, 22 h, 26 h, 30 h, 41 h, 48 h, 72 h) to assess community composition by 16S rRNA Illumina sequencing, and smaller aliquots (1 mL) were collected at the same sampling times to estimate cell concentration by flow cytometry (Fig. 1).

Table 1 Label and taxonomical affiliation of the strains making up the microbial community. Each percentage indicates the percentage of identity to closest hit

Strain label	Phylum (class)	Family	Closest hit SILVA	Closest hit BLAST	Oxygen requirement of closest hit BLAST	Color of colonies on R2-agar
78R	β-Proteobacteria	Oxalobacteraceae	*Janthinobacterium* sp. (99.58%)	*Janthinobacterium lividum* (98.16%)	Strictly aerobic [48]	Purple
124Z	α-Proteobacteria	Caulobacteraceae	*Brevundimonas* sp. (99.69%)	*Brevundimonas intermedia* (99.62%)	Strictly aerobic [49]	Orange
515Z	Bacteroidetes	Flavobacteraceae	*Flavobacterium* sp. (98.32%)	*Flavobacterium saccharophilum* (95.67%)	Strictly aerobic [6]	Yellow
1315Z	β-Proteobacteria	Comamonadaceae	*Variovorax* sp. (98.25%)	*Variovorax ginsengisoli* (97.27%)	Aerobic + facultatively anaerobic [50]	White

The growth of each individual strain in monoculture (three biological replicates) was run in the same conditions as mentioned above, and 1 mL-aliquots were collected at 23 sampling times (0 h, 16.5 h, 18 h, 19.5 h, 21 h, 22.5 h, 24 h, 25.5 h, 27 h, 28.5 h, 30 h, 40.5 h, 42 h, 43.5 h, 45 h, 46.5 h, 48 h, 64.5 h, 66 h, 67.5 h, 69 h, 70.5 h, 72 h) to assess cell concentration by flow cytometry.

DNA Extraction and Illumina Sequencing

Aliquots (25 to 50 mL) of each (co-)culture were collected in Falcon tubes and bacterial biomass was pelleted by centrifugation at 10,000 g and 4 °C for 15 min. Supernatants were discarded and pellets were kept at − 20 °C until DNA extraction. Genomic DNA extraction was performed with the DNeasy UltraClean Microbial Kit (Qiagen, Hilden, Germany) following the manufacturer's protocol. The concentration and purity of the extracts were estimated using a Nanodrop ND-2000 UV–vis spectrophotometer (Thermo Fisher Scientific, Waltham, US). The V4 region of the 16S rRNA gene was amplified with primers 515F (GTGYCAGCMGCC GCGGTAA) and 806bR (GGACTACNVGGGTWTCTAAT) and sequenced on an Illumina MiSeq sequencer at StarSEQ laboratory (Mainz, Germany) following a paired-end approach. Sequences were trimmed at 240 bp using Trimmomatic (http://www.usadellab.org/cms/?page=trimmomatic) and then processed with MOTHUR (https://mothur.org), following the MiSeq Standard Operating Procedure [36] (version 1.42.3 revised on 6/24/2019). Reads were assembled into contigs, and contigs shorter than 275 bp or containing ambiguous bases were removed from the dataset. Remaining contigs were aligned against the silva.nr_v138.align file trimmed to the V4 region, preclustered to decrease the number of sequences to only keep unique sequences, and screened for chimeras using the vsearch program. Remaining sequences (contigs) were classified with GreenGenes (version gg_13_8_99). Taxon counts were corrected for 16S rRNA gene copy number based on copy number for each genus (average value when several genomes were available) retrieved from the NCBI Nucleotide (https://www.ncbi.nlm.nih.gov/nuccore) and *rrn*DB (https://rrndb.umms.med.umich.edu) databases (in parallel), and then converted to relative abundances. Finally, absolute abundance of a given taxon was obtained by multiplying its relative abundance with the total bacterial count in the relevant sample determined with flow cytometry.

Bacterial Enumeration by Flow Cytometry

Samples (1 mL) were fixed with paraformaldehyde (3% final concentration), left for 15 min at 4 °C, and then stored frozen at − 20 °C. Prior to analysis, samples were serially tenfold diluted in 0.22 µm-filtered then autoclaved phosphate buffered saline, and cell counting was performed on two dilutions to target an ideal rate of 200 to 2,000 events/sec. Flow cytometry was performed according to the procedure described in [37] with slight modifications. Cells were stained with SYBR GREEN I (10,000-fold diluted from stock solution in 0.22 µm-filtered DMSO; Amresco, Solon, USA). They were then incubated for 20 min in the dark at 37 °C. Stained samples were inoculated in technical triplicate in a 96-deep-well microplate and analysed using an Accuri C6 flow cytometer (BD, Franklin Lakes, US) equipped with an auto-loader. Bacterial abundance (cells/mL) was calculated by counting fluorescent events in 400 µL after gating plots on the green (FL1) vs red (FL3) fluorescence. For each biological replicate, the growth curve was built from the mean bacterial abundance of the technical triplicates at each sampling time.

Interaction Matrices

The growth rate μ of a strain was estimated by calculating the slope of the straight line fitting the logarithmic (ln) growth curve in exponential phase. For monocultures, a time range between 16.5 and 30 h was selected to fit

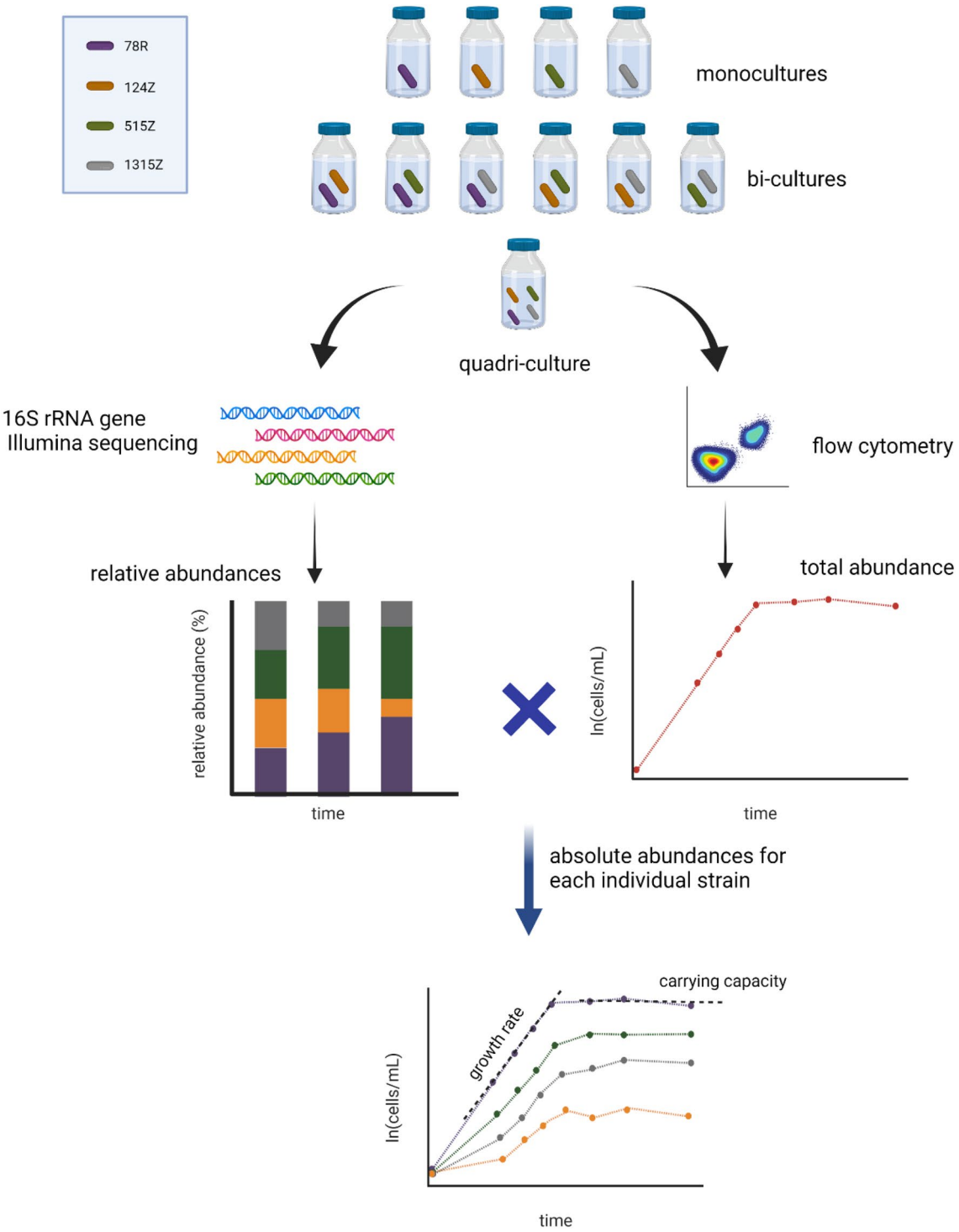

Fig. 1 Scheme summarizing the experimental set-up. Culture experiments and downstream analyses were performed in triplicate. Note that sequencing was not applied to monoculture samples. Created with BioRender.com

the exponential phase and calculate the growth rate. For bi- and quadri-cultures, a time range between 0 and 41 h (depending on the replicate) was taken to fit the exponential phase. The carrying capacity K was computed as the average cell concentration reached by the strain at the stationary phase over two to three time points. Details of time range used for fitting are available in Tables 2 and S1.

Table 2 Growth rate and carrying capacity values for each strain in monoculture. Bold values of μ and K are mean values, given with their standard deviation. The CV (coefficient of variation) is defined as the standard deviation divided by the mean value of μ or K, respectively. The goodness of fit refers to the line fitted to the exponential part of the natural logarithmic (ln) growth curve from all replicates pooled

Strain number	Growth rate μ (h^{-1})	CV (%)	Goodness of fit (R^2)	Time range for fitting μ	Carrying capacity K (cells/mL)	CV (%)	Time range for fitting K
78R	$\mathbf{0.57} \pm 0.01$	1.75	0.94	16.5 h – 25.5 h	$\mathbf{1.31 \times 10^9} \pm 2.81 \times 10^8$	21.50	40.5 h – 72 h
124Z	$\mathbf{0.25} \pm 0.01$	2.28	0.97	16.5 h – 48 h	$\mathbf{4.00 \times 10^9} \pm 1.21 \times 10^8$	3.03	64.5 h – 72 h
515Z	$\mathbf{0.42} \pm 0.01$	2.38	0.95	16.5 h – 30 h	$\mathbf{2.44 \times 10^9} \pm 5.26 \times 10^8$	21.54	40.5 h – 72 h
1315Z	$\mathbf{0.27} \pm 0.02$	7.41	0.93	16.5 h – 42 h	$\mathbf{7.96 \times 10^8} \pm 4.55 \times 10^8$	57.20	64.5 h – 72 h

Each μ and K final value is the mean value calculated on the three biological replicates.

The effect of a strain B on strain A's growth rate was quantified as follows:

$$\alpha = \ln\left(\frac{\mu_{\text{A in bi-culture A\_B}}}{\mu_{\text{A in monoculture}}}\right)$$

The effect of a strain B on strain A's carrying capacity was quantified as follows:

$$\kappa = \ln\left(\frac{K_{\text{A in bi-culture A\_B}}}{K_{\text{A in monoculture}}}\right)$$

The absolute value and the sign of α and κ indicate the strength and the type of the interaction (positive or negative), respectively. These calculations follow those presented in [19]. In order to obtain the value of α for strain A, each replicate of μ_A in bi-culture A_B was compared to each replicate of μ_A in monoculture, and the mean of these nine values was reported as α. The same procedure was applied for κ values. For quadri-cultures, the effect of three strains on the fourth was calculated as detailed above, replacing μ and K in bi-culture by μ and K in quadri-culture. We computed the standard deviations of α and κ across replicates for each strain pair and selected the maximal standard deviation across all strain pairs as a threshold (replicate 1 of pair 78R_124Z was excluded of the calculations because 515Z was detected at some time points and could have influenced the dynamics of that replicate). For an interaction to be considered significant, α and κ had to be larger than their respective threshold. For bi-cultures, the threshold for α was 0.163 and the threshold for κ was 1.899. For quadri-cultures, the threshold for α was 0.459 and the threshold for κ was 0.971 (Table S2).

Antagonism Tests

Antagonism tests were carried out as described in Marinho et al. [38] with modifications. Briefly, the liquid culture was inoculated after 24 h (exponential phase) or 48 h (stationary phase) of incubation (R2B, 20 °C, 176 rpm). Then, 3×10 µL of liquid culture of the strain that potentially produces antimicrobial substances (sampled in exponential or stationary phase to match the physiological state of the target strain) were inoculated on a R2-agar plate. Once the drops had penetrated the solid medium, they were covered by a thin layer of semi-solid agar (7.5 g/L) to avoid dispersion of the cells. Then, semi-solid medium (R2B added with 7.5 g/L of agar) mixed with the target strain was poured over the productive strain. After incubation at 20 °C for 24 h, production of antagonistic molecules could be assessed by the presence/absence of a zone of inhibition appearing above (and beyond the diameter of) the colony of the productive strain. These tests were carried out only in the bi-cultures 78R_124Z and 78R_1315Z (Table S3).

Oxygen Measurements

To quantify the extent to which oxygen is limiting in our experiments, we measured oxygen quantity and saturation in Schott bottles containing the quadri-culture in 1 L of R2B after 48 h of incubation. The measurements were carried out using an oxygen probe (VWR International, model DO 200) and following manufacturer's protocol. Three situations were tested: stirring at 20 °C and 176 rpm, no stirring at 20 °C, and no stirring at 20 °C with the addition of a bubbling device in the bottle. Each situation was performed in triplicate. An uninoculated bottle containing only 1 L of R2B was set up as negative control (Table S4).

Statistical Analysis

Pearson correlations were computed between the strength of interactions and the cell abundance of the target strain with function cor.test in R. Correlations were also computed between growth rates and carrying capacities, first in mono- versus co-culture, then all cultures considered (including a 20-strain mix from [39]). Significance was assessed with a t-test at confidence level 95%. P-values were corrected for multiple testing with Bonferroni. All

statistical tests were performed in R (https://cran.r-project.org) version 4.1.2.

Results

The Fastest Growing Strain in Monoculture, *Janthinobacterium* sp. 78R, Dominates the Co-cultures

We sampled mono-, bi- and the quadri-culture of the four selected river bacterial strains over 72 h, resolved the taxonomic composition in co-cultures with 16S rRNA gene sequencing and obtained total cell counts using flow cytometry (Fig. 2 and S3).

Individual growth rates of the strains ranged from 0.25 to 0.57 h^{-1} (Table 2). The two fastest growing strains were (in decreasing order) 78R and 515Z, and the two slowest ones were 1315Z and 124Z. Individual carrying capacities ranged from $\approx 8\times10^8$ to 4×10^9 cells/mL, with *Brevundimonas* sp. 124Z being the most productive strain, followed by 515Z, 78R and 1315Z being the least productive one.

In all bi-cultures except 78R_515Z (Fig. 2), one strain clearly dominated the other one in terms of production of cells. Moreover, the abundance of the dominant strain was less variable than the abundance of the dominated strain (CVs in Table S1). The order of dominance in bi-culture was not correlated to the carrying capacity in monoculture: 78R was always the most productive strain in each of its three bi-cultures, alike 515Z in bi-cultures 124Z_515Z and 515Z_1315Z. 1315Z, despite being the least productive in monoculture, dominated 124Z in bi-culture. Notably, *Brevundimonas* sp. 124Z was systematically the less productive one in bi-cultures. These results show that the carrying capacity in monoculture was not predictive of the order of dominance in bi-culture.

Of note, one biological replicate of 78R_124Z had to be discarded due to contamination, which leaves this bi-culture with two biological replicates. All other bi-cultures were studied with three biological replicates. Details of all α and κ values can be found in Table S2.

In the quadri-culture (Fig. S3), the relationship between dominant and dominated strains was reproduced in the three replicates: whether in exponential or stationary phase, 78R was the most abundant strain, followed by 515Z, 1315Z and 124Z. No strain was lost within the 72 h of incubation, *i.e.* there was no case of competitive exclusion in the time frame of this experiment.

Competition Dominates Interactions and Networks Differ from Exponential to Stationary Phase

In exponential growth phase (see time range for fitting μ in Table S1), there were three significant competitive interactions (negative effect in both ways) (Fig. 3a) (see Material and Methods for assessment of significance). *Janthinobacterium* sp. 78R was the only strain significantly negatively

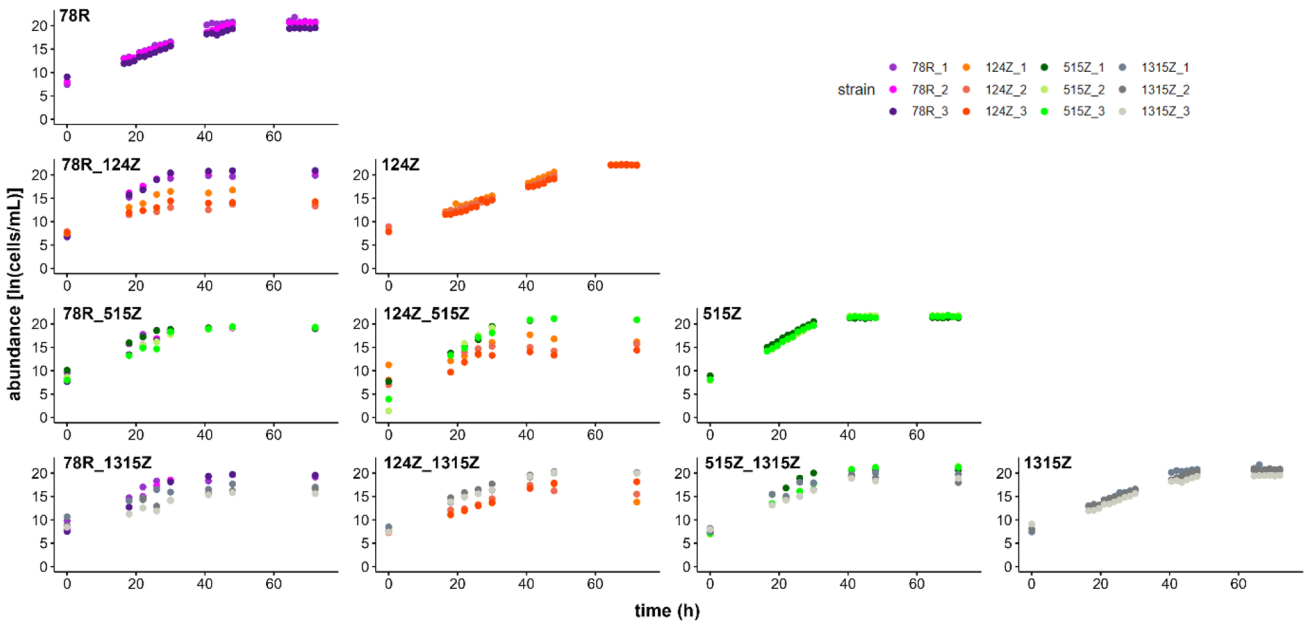

Fig. 2 Time series representing the dynamics of the monocultures (diagonal) and bi-cultures (lower triangle) over 72 h, with cell concentrations presented in natural logarithmic (ln) values. Each culture was carried out in triplicate. Bacterial abundances of each strain (y axis) were calculated as presented in Fig. 1

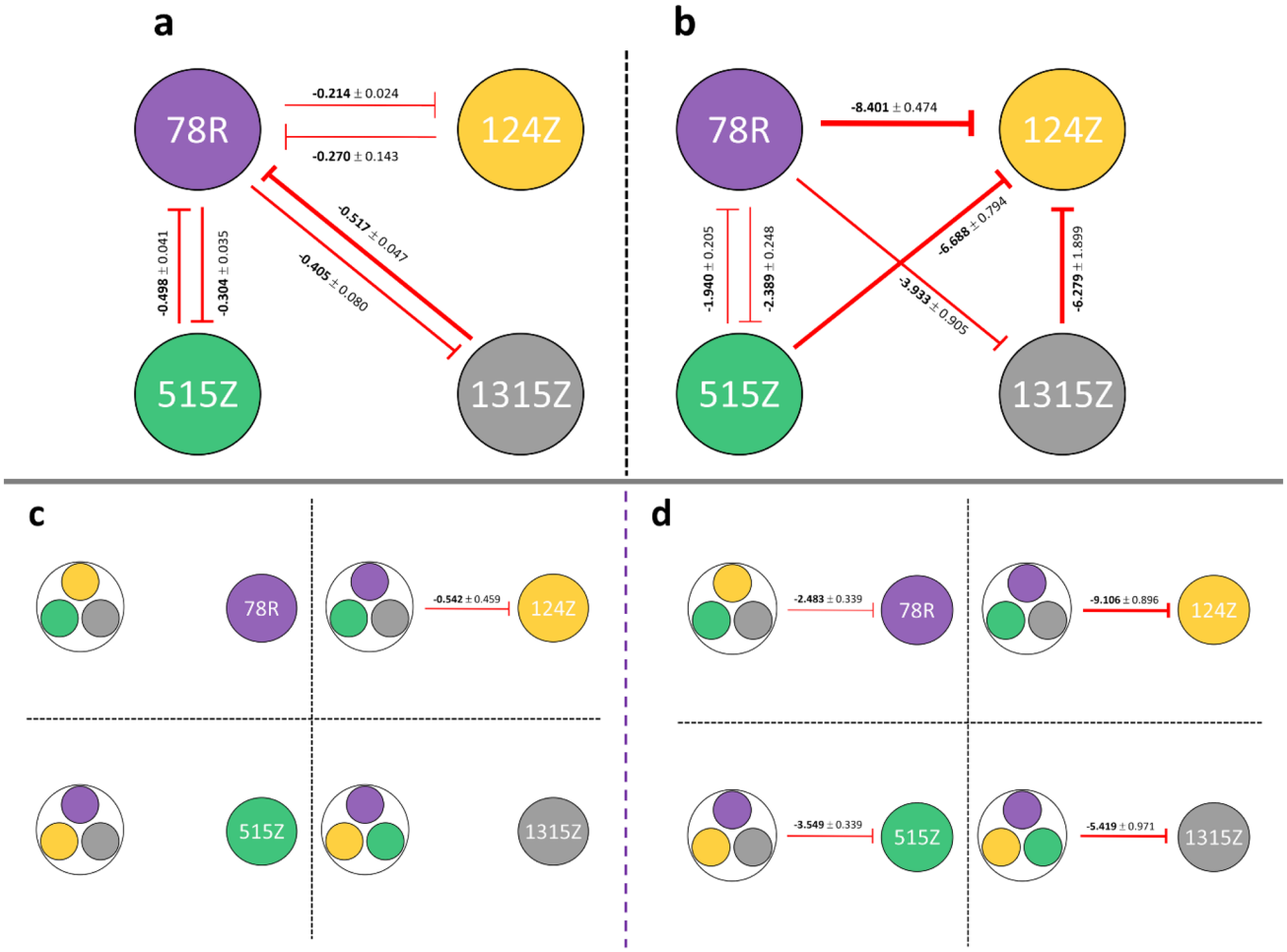

Fig. 3 Interaction networks showing interactions measured in bi-cultures (top) and quadri-culture (bottom). Top part of the figure shows pairwise interactions obtained from comparison of growth rates (exponential phase) (**a**) and carrying capacities (stationary phase) (**b**) in bi-cultures versus monocultures. Bottom part of the figure shows interactions between each strain and the rest of the community, obtained from comparison of growth rates (**c**) and carrying capacities (**d**) in quadri-culture versus monocultures. Red arcs indicate a negative interaction. Arc thickness reflects the absolute value of the mean of α and κ, which is also given in bold indicated with its respective standard deviation. For interactions in bi-cultures (**a** and **b**), only α and κ values above the threshold of, respectively, 0.163 and 1.899 are represented. For interactions in quadri-culture (**c** and **d**), only α and κ values above the threshold of, respectively, 0.459 and 0.971 are represented (see Methods for threshold calculation) (Color figure online)

affected in each of its three bi-cultures, and negatively affecting each of its partners.

In stationary phase (see time range for fitting K in Table S1), all five significant interactions were negative (Fig. 3b), with one case of competition (78R_515Z), and four cases of amensalism (negative effect in one way). In the competition case, the negative effect on both strains was less intense compared to exponential phase, whereas the most negatively affected strain in stationary phase was *Brevundimonas* sp. 124Z. In addition, the second most affected strain was *Variovorax* sp. 1315Z, highlighting that the two slowest growing strains were the most affected ones regarding carrying capacity. This network shows that carrying capacity could be affected without the growth rate being changed, as it was the case for bi-cultures 124Z_515Z, 124Z_1315Z and 515Z_1315Z.

In the quadri-culture, only one interaction was detected in exponential phase, namely amensalism towards *Brevundimonas* sp. 124Z by the three other strains (Fig. 3c). In stationary phase, the interaction network only contained amensalistic negative values. The strength of the amensalistic interactions was negatively correlated to cell abundance of the target strain (Pearson correlation test, $n = 4$, $R = -0.97$, $P = 0.03$). In fact, all co-cultures considered, the strength of the negative interactions (competitive plus amensalistic) was negatively correlated to cell abundance of the target strain (Pearson correlation test, $n = 16$, $R = -0.94$, $P = 4 \times 10^{-8}$). As for bi-cultures, interaction networks constructed for both phases revealed

differences that highlight the importance of studying interactions in different growth phases.

The Slowest Growing Strain (124Z) Inhibits the Growth of the Fastest Growing One (78R) in Antagonism Tests

To unravel the nature of interactions in bi-cultures where the growth rate of the dominant strain was affected by a partner strain being 10 to 100 times less abundant (either in exponential or stationary phase), we tested pairs of strains 78R_124Z and 78R_1315Z for antagonistic relationships in double layer agar plates. Antagonism tests detected only one case of antibacterial activity, namely *Brevundimonas* sp. 124Z inhibiting *Janthinobacterium* sp. 78R (Table S3). This activity was more intense (wider zone of inhibition) when both strains were inoculated in exponential phase than in stationary phase.

Growth Rate Correlates with Carrying Capacity in Co-cultures

Growth rate in monoculture was significantly positively correlated with carrying capacity in bi-culture and quadri-culture (Fig. 4a). Plus, this plot highlights the greater variability in carrying capacity of the slowest growing strains (124Z and 1315Z) compared to the fastest growing ones (78R and 515Z) in both types of co-cultures.

Similarly, growth rates in co-cultures were significantly positively correlated with carrying capacities in co-cultures (Fig. 4b), whereas no such correlation was observed in monocultures ($R = -0.18$, $P = 0.82$). This result indicates that there was no trade-off between growth rate and carrying capacity in co-cultures. In addition, we compared the μ and K values of each strain in the mono-, bi-, quadri- and 20-strain cultures (Fig. 5). Of note, growth rates tended to decrease with the number of strains present in the culture, but were all higher in the 20-strain mix (data retrieved from [39]) than in the quadri-culture (Fig. 5), except for *Janthinobacterium* sp. 78R. Carrying capacities followed the same trend.

Discussion

In this study, we followed the dynamics of river bacterial strains individually in multi-strain cultures and combined 16S rRNA sequencing and flow cytometry to measure growth rates and carrying capacities. These two parameters led to the construction of interaction networks which differed in the exponential and stationary growth phase.

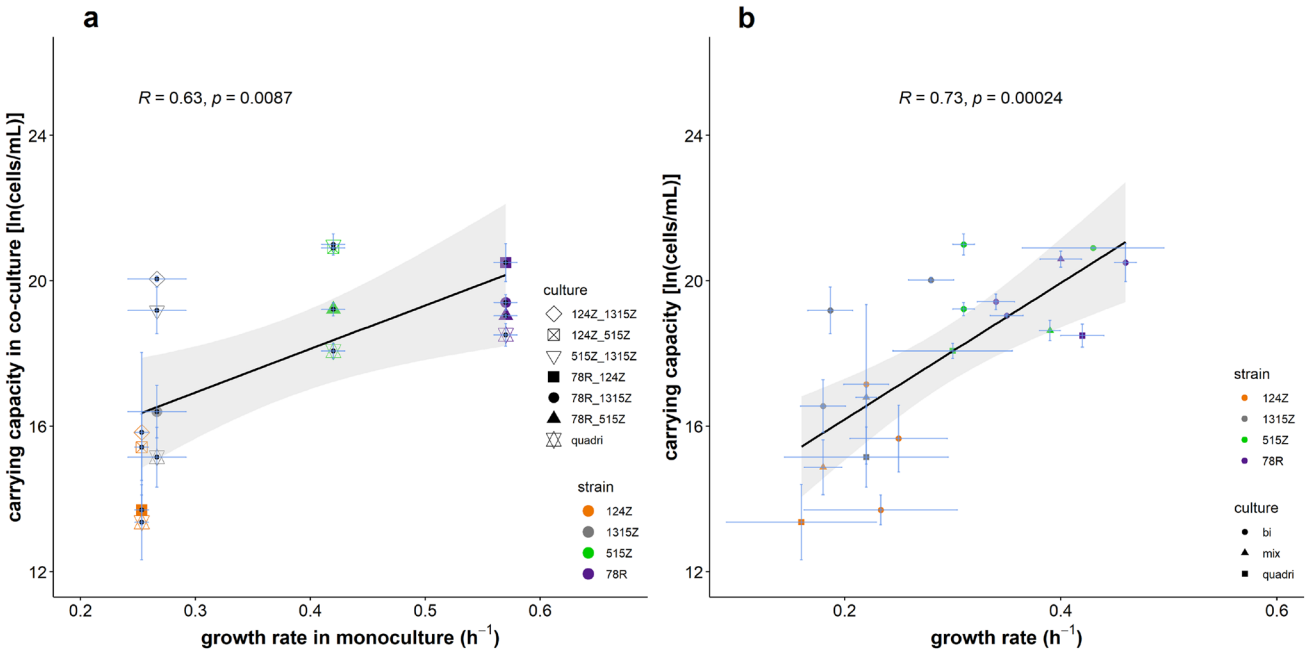

Fig. 4 Comparison of growth rate and carrying capacity values. Panel (**a**) compares growth rate in monoculture to carrying capacity in co-culture, and panel (**b**) compares growth rate to carrying capacity in three types of multi-strain cultures: bi-culture, quadri-culture and mix. The mix refers to a co-culture of 20 strains studied by Goetghebuer et al. [39] which included the 4 strains used in this study. Values R and p refer, respectively, to Pearson's correlation coefficient and associated p-value. The light grey zone indicates a 95% confidence interval (Color figure online)

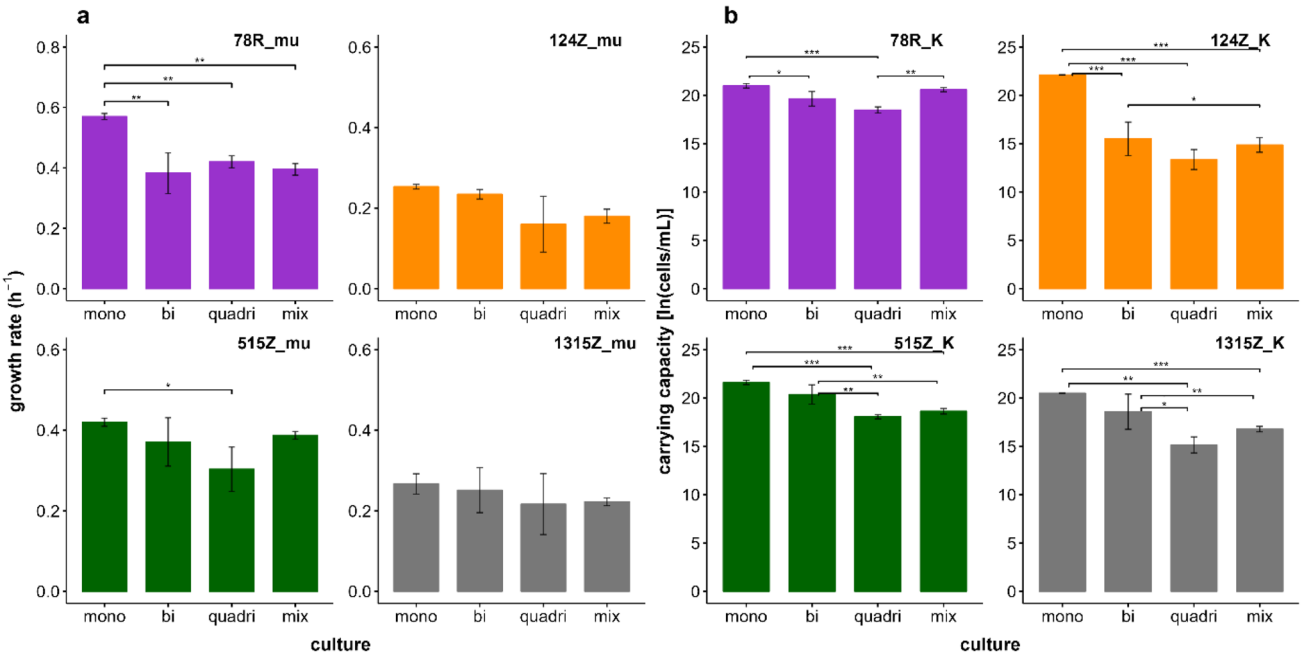

Fig. 5 Barplots showing mean growth rates (**a**) and mean carrying capacities (**b**) versus type of culture (mono = monoculture, bi = bi-culture, quadri = quadri-culture, mix = community of 20 strains). Error bars correspond to standard deviations across three biological replicates of the same (co-)culture, except for bi-cultures where they correspond to standard deviations across the mean values of the three different bi-cultures. Brackets over two bars correspond to unpaired Student tests giving a significative p-value: $P < 0.05$ (*), $P < 0.01$ (**) or $P < 0.001$ (***), after applying Bonferroni's correction for multiple comparisons. Non-significant p-values are not shown. The data used to plot the bars corresponding to "mix" come from the study conducted by Goetghebuer et al. [39]

Previously published data from a 20-taxa riverine community containing our four strains [21, 39] already suggested the presence of interactions, but without studying pairwise interactions. Our results show that this microbial community constitutes a globally competitive system: neither in the bi-cultures (Fig. S1 and S2) nor in the quadri-culture (Fig. S2 and S3), did the total cell counts reach higher values than in monocultures. There was no case of increased growth rate nor carrying capacity in bi- or quadri-culture compared to monocultures (Fig. 5); in other words, we did not infer any positive interaction (Fig. 3). The fact that competition dominates interspecies interactions at stationary phase has been observed in aquatic communities previously [40] as well as in a nutrient-rich and homogenized medium [41]. The choice of the strains composing the synthetic community is an additional factor that can drive interactions towards competitions [42]. In this system, growth rate in monoculture was predictive of carrying capacity in co-culture (Fig. 4a), as expected in a system dominated by competition where strains compete for the same resources. One likely limiting resource in our experimental set-up is oxygen, which is rapidly depleted (oxygen saturation drops to 5.4% after 48 h of incubation, see Table S4), therefore constituting a potential stress for the bacteria in culture.

The absence of trade-off between growth rate and carrying capacity in this system is consistent with observations in other communities originating from different environments such as soil [22] or human gut [20]. In the present study, the positive correlation between μ and K was observed in a well-mixed planktonic environment, in which resources are limited and not renewed (batch). The absence of a trade-off is expected in these conditions, as reviewed by Lipson [43] who theorized a relationship between μ and K across a broad range of environmental conditions and ecological strategies.

Higher-order interactions (HOIs), *i.e.* the impact of a third species on the interaction of two species, are a well-known limitation when attempting to describe community dynamics in terms of pairwise interactions [44]. When comparing interaction networks derived from bi- and quadri-culture, the effect of HOIs is apparent here. For instance, the combined effect of 78R, 1315Z and 515Z on 124Z in quadri-culture in stationary phase (Fig. 3d) is much weaker than the sum of their negative impacts on 124Z in bi-culture (Fig. 3b).

Janthinobacterium sp. 78R is the most competitive strain in our microbial community: it has the highest growth rate in monoculture (Table 2) and mixed cultures, and the highest carrying capacity in mixed cultures (Fig. 5b). By reaching large abundances more quickly, thereby depleting metabolites that they are competing for, 78R may keep the abundance of the competitor low, thus reducing its negative impact on 78R in turn. This mechanism may also explain 78R's negative effect on other strains. *Janthinobacterium* is

a generalist, having the largest metabolic profile among the strains composing the microbial community [21]. It is also the only strain able to degrade nucleotides [21], a useful capacity in stationary phase when there are few nutrients left and nucleotides can be released in the environment from dead cells. When oxygen becomes limiting in the environment, even if other strains may cope better than 78R in such conditions (*e.g.* 1315Z, Table 1), it could be already too late for them to overtake 78R because there are not enough nutrients left. Although resource depletion is suspected to be the main driver of 78R's success in competition, interference competition is another possibility. Indeed, this bacterium synthesizes violacein, a violet pigment (Table 1) which is known to play a role in response to environmental stress [45] and cell survival [34]. Since 78R reaches stationary phase earlier than other strains, it is able to produce secondary metabolites sooner (such as violacein) that, added to nutrient depletion, can constitute a complementary strategy to dominate the rest of the community.

Interestingly, *Brevundimonas* sp. 124Z did not reach large abundances in bi-culture with *Janthinobacterium* sp. 78R (it had 100 times fewer cells) but it nevertheless greatly reduced 78R's growth rate compared to the monoculture. This behaviour is hard to capture with population models that assume a linear dependency of interaction strength to the abundance of other species. We were indeed unable to fit the generalized Lotka-Volterra model [19] to the experimental time series in bi-cultures. This limitation is likely due to the presence of non-additive, non-linear interaction terms. Such terms could take the form of HOIs or be saturated functions of nutrients (Monod function). Designing and fitting such models would, however, require additional information that were not measured in the present study (dynamics of nutrients, dependence of growth rates on the abundance of other species).

Antagonism tests in agar plates (Table S3) showed that *Brevundimonas* sp. 124Z inhibits *Janthnobacterium* sp. 78R, with stronger intensity in exponential than stationary phase. This could explain why we observed a negative effect of 124Z on 78R in exponential phase (despite the difference in cell concentration), which does not appear in the network in stationary phase (Fig. 3b). It is also remarkable that 124Z was the only strain whose exponential phase is much shorter in co-culture (stops around $t = 30$ h, lower triangle in Fig. 2) than in monoculture (lasts until $t = 48$ h, diagonal in Fig. 2). This shortening could be caused by the decrease of an important resource in the medium. For instance, oxygen depletion rate may be different in co- than in monoculture, as already observed elsewhere [46]. The depletion of carbon sources in co-culture could also greatly affect 124Z more than others because 124Z is a specialist [21]. These hypotheses are supported by the fact that these two parameters have already been reported to predict decreased K at low growth rate and low substrate concentrations [47]. Thus, when modelling batch dynamics, both interaction-dependent growth rates and interaction-dependent carrying capacities need to be taken into account, as recently done by de Vos and colleagues [19].

Conclusion

In this study, we built an experimental set-up that allowed sampling of mono-, bi- and quadri-cultures over 72 h to calculate two key parameters, *i.e.* growth rate and carrying capacity. These were used to measure pairwise interactions between each pair of strains in bi-culture, and between each strain and the rest of the community in quadri-culture, both in exponential and stationary phases. Resulting interaction networks showed significant differences, which highlight the importance of taking these two growth phases into account when measuring interactions in time series experiments, as well as for parametrizing growth models from such experimental data. Moreover, the growth rate of the dominant strain was negatively affected by the presence of strains much less abundant in the bi-cultures.

In this system, the winner of the competition could be expected based on its high growth rate compared to the other strains. Since the relationship between μ or K and the number of strains in the co-culture may not be linear (Fig. 5), it would be interesting to study how these values scale with species number. The winner of the competition could also be expected based on its generalist metabolic profile combined to the complex nature of the growth medium (R2B). The next relevant step of investigation would be to explore how altering conditions, such as varying the quality and quantity of the carbon sources in the medium or stress, affect interactions between these strains. Studying interactions between river bacteria in the context of such perturbations would help understand how they respond to organic pollution.

Supplementary Information The online version contains supplementary material available at https://doi.org/10.1007/s00284-023-03342-9.

Acknowledgements The authors thank Adriana Anzil for her contribution to the experimental work, and Pierre Servais for his feedback on the scientific project.

Author Contributions MB, DG, KF and IFG: contributed to the study conception and design. LG: sampled and isolated the bacterial strains used in this study. CJ: contributed to flow cytometry data analysis. MB: carried out the experiments. MB, DG, KF and IFG: analysed the data. MB: wrote the manuscript and all authors commented on previous versions, read and approved the final version.

Funding This work was supported by a PhD grant to M. Bonal from the Fonds de la Recherche dans l'Industrie et l'Agriculture (FRIA) at

the Fonds de la Recherche Scientifique (FRS-FNRS), as well as by a FRS-FNRS project (DYNAMO T.1037.14), in Belgium.

Data Availability The datasets generated and analysed during the current study are available from the corresponding author on reasonable request. The NCBI BioProject ID containing information and sequences about the strains used in this study is PRJNA832615.

Code Availability The analysis pipeline used to create Figs 2, 4, 5, S1 and S2 is available as an R document at https://github.com/Mathias-Bonal/Four-strain_community.

Declarations

Conflict of interest The authors have no relevant financial or non-financial interests to disclose.

Ethical Approval Not applicable

Consent to Participate Not applicable

Consent for Publication Not applicable

References

1. Amon RM, Benner R (1996) Bacterial utilization of different size classes of dissolved organic matter. Limnol Oceanogr 41:41–51. https://doi.org/10.4319/lo.1996.41.1.0041
2. Billen G, Servais P, Bianchi M (1989) Modélisation des processus de dégradation bactérienne de la matière organique en milieu aquatique. Micro-organismes dans les écosystèmes océaniques, 219–245
3. Hosen JD, Febria CM, Crump BC, Palmer MA (2017) Watershed urbanization linked to differences in stream bacterial community composition. Front Microbiol 8:1452. https://doi.org/10.3389/fmicb.2017.01452
4. Staley C, Unno T, Gould TJ et al (2013) Application of Illumina next-generation sequencing to characterize the bacterial community of the Upper Mississippi River. J Appl Microbiol 115:1147–1158. https://doi.org/10.1111/jam.12323
5. Zeglin LH (2015) Stream microbial diversity in response to environmental changes: review and synthesis of existing research. Front Microbiol 6:454. https://doi.org/10.3389/fmicb.2015.00454
6. Bernardet J-F, Segers P, Vancanneyt M et al (1996) Cutting a gordian knot: emended classification and description of the genus *flavobacterium*, emended description of the family Flavobacteriaceae, and proposal of *Flavobacterium hydatis* nom. nov. (Basonym, *Cytophaga aquatilis* Strohl and Tait 1978). Int J Syst Evol Microbiol 46:128–148. https://doi.org/10.1099/00207713-46-1-128
7. Dejonghe W, Berteloot E, Goris J et al (2003) Synergistic degradation of linuron by a bacterial consortium and isolation of a single Linuron-degrading *Variovorax* Strain. Appl Environ Microbiol 69:1532–1541. https://doi.org/10.1128/AEM.69.3.1532-1541.2003
8. Faust K, Raes J (2012) Microbial interactions: from networks to models. Nat Rev Microbiol 10:538–550. https://doi.org/10.1038/nrmicro2832
9. Kurtz ZD, Müller CL, Miraldi ER et al (2015) Sparse and compositionally robust inference of microbial ecological networks. PLOS Comput Biol 11:e1004226. https://doi.org/10.1371/journal.pcbi.1004226
10. Stein RR, Bucci V, Toussaint NC et al (2013) Ecological modeling from time-series inference: insight into dynamics and stability of intestinal microbiota. PLOS Comput Biol. 9:e1003388. https://doi.org/10.1371/journal.pcbi.1003388
11. Buffie CG, Bucci V, Stein RR et al (2015) Precision microbiome reconstitution restores bile acid mediated resistance to *Clostridium difficile*. Nature 517:205–208. https://doi.org/10.1038/nature13828
12. Lima-Mendez G, Faust K, Henry N et al (2015) Ocean plankton. Determinants of community structure in the global plankton interactome. Science 348:1262073. https://doi.org/10.1126/science.1262073
13. Hirano H, Takemoto K (2019) Difficulty in inferring microbial community structure based on co-occurrence network approaches. BMC Bioinformatics 20:329. https://doi.org/10.1186/s12859-019-2915-1
14. Weiss S, Van Treuren W, Lozupone C et al (2016) Correlation detection strategies in microbial data sets vary widely in sensitivity and precision. ISME J 10:1669–1681. https://doi.org/10.1038/ismej.2015.235
15. Gause GF (1934) The struggle for existence. The Williams & Wilkins company, Baltimore
16. Gould AL, Zhang V, Lamberti L et al (2018) Microbiome interactions shape host fitness. Proc Natl Acad Sci 115:E11951–E11960. https://doi.org/10.1073/pnas.1809349115
17. Lawrence D, Fiegna F, Behrends V et al (2012) Species interactions alter evolutionary responses to a novel environment. PLOS Biol 10:e1001330. https://doi.org/10.1371/journal.pbio.1001330
18. Ram Y, Dellus-Gur E, Bibi M et al (2019) Predicting microbial growth in a mixed culture from growth curve data. Proc Natl Acad Sci 116:14698–14707. https://doi.org/10.1073/pnas.1902217116
19. de Vos MGJ, Zagorski M, McNally A, Bollenbach T (2017) Interaction networks, ecological stability, and collective antibiotic tolerance in polymicrobial infections. Proc Natl Acad Sci 114:10666–10671. https://doi.org/10.1073/pnas.1713372114
20. Venturelli OS, Carr AV, Fisher G et al (2018) Deciphering microbial interactions in synthetic human gut microbiome communities. Mol Syst Biol 14:e8157. https://doi.org/10.15252/msb.20178157
21. Goetghebuer L, Servais P, George IF (2017) Carbon utilization profiles of river bacterial strains facing sole carbon sources suggest metabolic interactions. FEMS Microbiol Lett. https://doi.org/10.1093/femsle/fnx098
22. Friedman J, Higgins LM, Gore J (2017) Community structure follows simple assembly rules in microbial microcosms. Nat Ecol Evol 1:1–7. https://doi.org/10.1038/s41559-017-0109
23. Stevenson K, McVey AF, Clark IBN et al (2016) General calibration of microbial growth in microplate readers. Sci Rep 6:38828. https://doi.org/10.1038/srep38828
24. Heyse J, Buysschaert B, Props R et al (2019) Coculturing bacteria leads to reduced phenotypic heterogeneities. Appl Environ Microbiol 85:13. https://doi.org/10.1128/AEM.02814-18
25. Piccardi P, Vessman B, Mitri S (2019) Toxicity drives facilitation between 4 bacterial species. Proc Natl Acad Sci 116:15979–15984. https://doi.org/10.1073/pnas.1906172116
26. Coyte KZ, Schluter J, Foster KR (2015) The ecology of the microbiome: Networks, competition, and stability. Science 350:663–666. https://doi.org/10.1126/science.aad2602
27. Gonze D, Lahti L, Raes J, Faust K (2017) Multi-stability and the origin of microbial community types. ISME J 11:2159–2166. https://doi.org/10.1038/ismej.2017.60
28. Sloan WT, Nnaji CF, Lunn M et al (2021) Drift dynamics in microbial communities and the effective community size. Environ Microbiol 23:2473–2483. https://doi.org/10.1111/1462-2920.15453
29. García-Armisen T, İnceoğlu Ö, Ouattara NK et al (2014) Seasonal variations and resilience of bacterial communities in a sewage

polluted urban river. PLOS ONE 9:e92579. https://doi.org/10.1371/journal.pone.0092579
30. Ghai R, Rodríguez-Valera F, McMahon KD et al (2011) Metagenomics of the water column in the pristine upper course of the Amazon river. PLOS ONE 6:e23785. https://doi.org/10.1371/journal.pone.0023785
31. Adhikari NP, Liu Y, Liu K et al (2019) Bacterial community composition and diversity in Koshi River, the largest river of Nepal. Ecol Indic 104:501–511. https://doi.org/10.1016/j.ecolind.2019.05.009
32. Read DS, Gweon HS, Bowes MJ et al (2015) Catchment-scale biogeography of riverine bacterioplankton. ISME J 9:516–526. https://doi.org/10.1038/ismej.2014.166
33. Satola B, Wübbeler JH, Steinbüchel A (2013) Metabolic characteristics of the species *Variovorax paradoxus*. Appl Microbiol Biotechnol 97:541–560. https://doi.org/10.1007/s00253-012-4585-z
34. Pantanella F, Berlutti F, Passariello C et al (2007) Violacein and biofilm production in *Janthinobacterium lividum*. J Appl Microbiol 102:992–999. https://doi.org/10.1111/j.1365-2672.2006.03155.x
35. Corno G, Coci M, Giardina M et al (2014) Antibiotics promote aggregation within aquatic bacterial communities. Front Microbiol 5:297. https://doi.org/10.3389/fmicb.2014.00297
36. Kozich JJ, Westcott SL, Baxter NT et al (2013) Development of a dual-index sequencing strategy and curation pipeline for analyzing amplicon sequence data on the miseq illumina sequencing platform. Appl Environ Microbiol 79:5112–5120. https://doi.org/10.1128/AEM.01043-13
37. Van Nevel S, Buysschaert B, De Roy K et al (2017) Flow cytometry for immediate follow-up of drinking water networks after maintenance. Water Res 111:66–73. https://doi.org/10.1016/j.watres.2016.12.040
38. Marinho PR, Moreira APB, Pellegrino FLPC et al (2009) Marine *Pseudomonas putida*: a potential source of antimicrobial substances against antibiotic-resistant bacteria. Mem Inst Oswaldo Cruz 104:678–682. https://doi.org/10.1590/s0074-02762009000500002
39. Goetghebuer L, Bonal M, Faust K et al (2019) The dynamic of a river model bacterial community in two different media reveals a divergent succession and an enhanced growth of most strains compared to monocultures. Microb Ecol 78:313–323. https://doi.org/10.1007/s00248-019-01322-w
40. Foster KR, Bell T (2012) Competition, not cooperation, dominates interactions among culturable microbial species. Curr Biol 22:1845–1850. https://doi.org/10.1016/j.cub.2012.08.005
41. Ghoul M, Mitri S (2016) The ecology and evolution of microbial competition. Trends Microbiol 24:833–845. https://doi.org/10.1016/j.tim.2016.06.011
42. Großkopf T, Soyer OS (2014) Synthetic microbial communities. Curr Opin Microbiol 18:72–77. https://doi.org/10.1016/j.mib.2014.02.002
43. Lipson DA (2015) The complex relationship between microbial growth rate and yield and its implications for ecosystem processes. Front Microbiol 6:615. https://doi.org/10.3389/fmicb.2015.00615
44. Billick I, Case TJ (1994) Higher order interactions in ecological communities: what are they and how can they be detected? Ecology 75:1529–1543. https://doi.org/10.2307/1939614
45. Matz C, Deines P, Boenigk J et al (2004) Impact of violacein-producing bacteria on survival and feeding of bacterivorous nanoflagellates. Appl Environ Microbiol 70:1593–1599. https://doi.org/10.1128/AEM.70.3.1593-1599.2004
46. Bor B, Poweleit N, Bois JS et al (2016) Phenotypic and physiological characterization of the epibiotic interaction between TM7x and its basibiont *Actinomyces*. Microb Ecol 71:243–255. https://doi.org/10.1007/s00248-015-0711-7
47. Van Bodegom P (2007) Microbial maintenance: a critical review on its quantification. Microb Ecol 53:513–523. https://doi.org/10.1007/s00248-006-9049-
48. Friedrich I, Hollensteiner J, Schneider D et al (2020) First complete genome sequences of *Janthinobacterium lividum* EIF1 and EIF2 and their comparative genome analysis. Genome Biol Evol 12:1782–1788. https://doi.org/10.1093/gbe/evaa148
49. Abraham W-R, Strömpl C, Meyer H et al (1999) Phylogeny and polyphasic taxonomy of *Caulobacter* species. Proposal of *Maricaulis* gen. nov. with *Maricaulis maris* (Poindexter) comb. nov. As the type species, and emended description of the genera *Brevundimonas* and *Caulobacter*. Int J Syst Evol Microbiol 49:1053–1073. https://doi.org/10.1099/00207713-49-3-1053
50. Im W-T, Liu Q-M, Lee K-J et al (2010) *Variovorax ginsengisoli* sp. nov., a denitrifying bacterium isolated from soil of a ginseng field. Int J Syst Evol Microbiol 60:1565–1569. https://doi.org/10.1099/ijs.0.014514-0